

## *Nitrogen seeding for heat load control in JET ELMy H-mode plasmas and its compatibility with ILW materials*

C. Giroud<sup>1</sup>, G. Maddison<sup>1</sup>, S. Jachmich<sup>2</sup>, F. Rimini<sup>1</sup>, M. Beurskens<sup>1</sup>, I. Balboa<sup>1</sup>, S. Brezinsek<sup>3</sup>, R. Coelho<sup>4</sup>, J.W. Coenen<sup>3</sup>, L. Frassinetti<sup>5</sup>, E. Joffrin<sup>6</sup>, M. Oberkofler<sup>7</sup>, M. Lehnen<sup>3</sup>, Y. Liu<sup>8</sup>, S. Marsen<sup>7</sup>, K. McCormick<sup>7</sup>, A. Meigs<sup>1</sup>, R. Neu<sup>7</sup>, B. Sieglin<sup>7</sup>, G. van Rooij<sup>9</sup>, G. Arnoux<sup>1</sup>, P. Belo<sup>4</sup>, M. Brix<sup>1</sup>, M. Clever<sup>3</sup>, I. Coffey<sup>10</sup>, S. Devaux<sup>7</sup>, D. Douai<sup>6</sup>, T. Eich<sup>7</sup>, J. Flanagan<sup>1</sup>, S. Grünhagen<sup>1</sup>, A. Huber<sup>3</sup>, M. Kempenaars<sup>1</sup>, U. Kruezi<sup>3</sup>, K. Lawson<sup>1</sup>, P. Lomas<sup>1</sup>, C. Lowry<sup>11</sup>, I. Nunes<sup>4</sup>, A. Sirinnelli<sup>1</sup>, A.C.C. Sips<sup>11</sup>, M. Stamp<sup>1</sup>, S. Wiesen<sup>3</sup> and JET-EFDA contributors\*

*JET-EFDA, Culham Science Centre, Abingdon, OX14 3DB, UK.*

<sup>1</sup>*EURATOM/CCFE Fusion Association, Culham Science Centre, Abingdon, Oxon. OX14 3DB, UK.*

<sup>2</sup>*Association Euratom-Etat Belge, ERM-KMS, Brussels Belgium.*

<sup>3</sup>*IEK-Plasmaphysik, Forschungszentrum Jülich, Association EURATOM-FZJ, Jülich, Germany.*

<sup>4</sup>*IPFN, EURATOM-IST Associação, 1096 Lisbon, Portugal.*

<sup>5</sup>*Association EURATOM-VR, Department of Physics, SCI, KTH, SE-10691 Stockholm, Sweden.*

<sup>6</sup>*CEA-Cadarache, Association Euratom-CEA, 13108 St Paul-lez-Durance France.*

<sup>7</sup>*Max-Planck-Institut für Plasmaphysik, EURATOM-Association, 85748 Garching, Germany.*

<sup>8</sup>*Institute of Plasma Physics, Chinese Academy of Sciences, Hefei 230031, China.*

<sup>9</sup>*Association EURATOM-FOM, PO BOX 1207, 3430 BE Nieuwegein, The Netherlands.*

<sup>10</sup>*Astrophysics Research Centre, Queen's University, Belfast, BT7 1NN, Northern Ireland, UK.*

<sup>11</sup>*JET-EFDA/CSU, Culham Science Centre, Abingdon, OX14 3DB, U.K.*

\**see Appendix of F Romanelli et al, Fusion Energy (24<sup>th</sup> IAEA Fusion Energy Conference 2012, San Diego, US*

*Email:carine.giroud@ccfe.ac.uk*

**Abstract:** *This paper reports the impact on the high-shape 2.5MA ELMy H-mode scenario at JET of a change from an all carbon plasma facing components to an all metal wall. In preparation to this change, systematic studies of power load reduction and impact on confinement as a result of fuelling in combination with nitrogen seeding were carried out in JET-C and are compared to their counterpart in JET with a metallic wall. An unexpected and significant change is reported on the decrease of the pedestal confinement but is partially recovered with the injection of nitrogen.*

### **1. Introduction**

The reference scenario for achieving  $Q=10$  in ITER is the type-I ELMy H-mode at 15MA, with a deuterium-tritium mixture, sufficient energy confinement ( $H_{98(y,2)} \sim 1$ ), at high density ( $f_{GDL} \sim 0.85$ ) and compatible with its Plasma Facing Components (PFCs). The expected power to the divertor makes high divertor radiation mandatory and requires the injection of extrinsic impurities. The challenge of achieving the scenario requirements with the material selection of the DT phase of ITER is being addressed at JET with its new wall (JET-ILW) plus main-chamber limiters made of bulk beryllium (Be) and a full tungsten (W) divertor [1]. Three aspects require investigation: first the capacity to reduce the inter-ELM power load to the divertor without significant degradation of the energy confinement; second the limitation of impurity production from the new PFCs to maintain performance, in terms of dilution (Be) and core radiation (W), the latter by reducing the target plasma temperature which governs the W sputtering yield; third the compatibility of the extrinsic impurities with the ILW materials in particular in the case of a chemically reactive specie such as  $N_2$  [2]. This paper investigates the first two aspects and in particular the potential of  $N_2$  seeding for achieving a radiative divertor for heat load control in JET.

## 2. Description of experiments and main results from JET-C seeding studies

With a change in JET of surface material from carbon phase (JET-C) to JET-ILW, a dramatic reduction in plasma C concentration was expected and a lower divertor radiation, as C strongly radiates in the temperature range characteristic of the divertor.

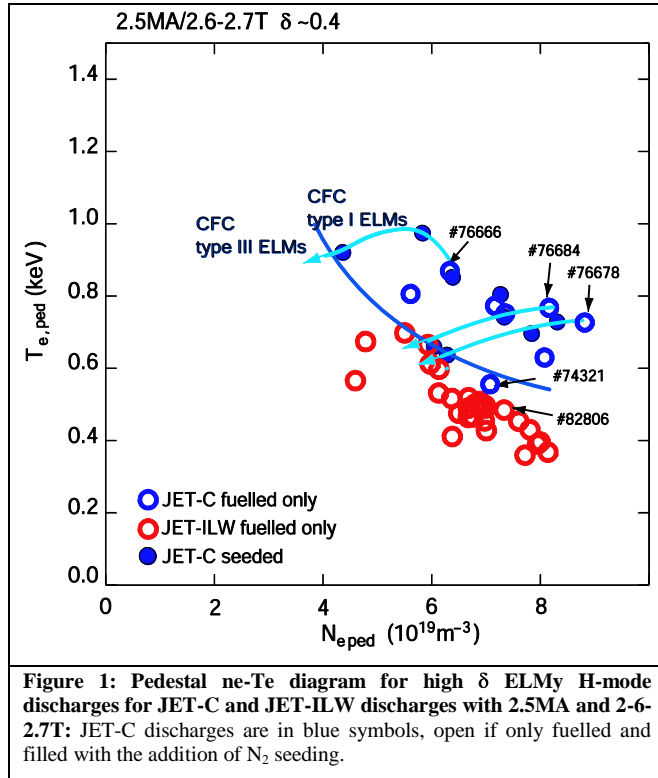


Figure 1: Pedestal ne-Te diagram for high  $\delta$  ELMy H-mode discharges for JET-C and JET-ILW discharges with 2.5MA and 2-6-2.7T: JET-C discharges are in blue symbols, open if only fuelled and filled with the addition of  $N_2$  seeding.

In preparation to document this change and its impact on power load to the divertor, experiments in JET-C explored the reduction of the inter-ELM power load in an ELMy H-mode scenario (2.7T/2.5MA,  $q_{95} \sim 3.5$ ,  $P_{in} \sim 16$  MW,  $\delta \sim 0.4$ ,  $H_{98(y,2)} \sim 1$ ,  $f_{rad} \sim 0.45$ ) at high density ( $f_{GDL} \sim 0.8$ ) with a fuelling mix of  $D_2$  and either Ne or  $N_2$ , constant input power and close to the transition from type I to III ELMs [3,4], see Figure 1. A deuterium fuelling scan from  $0.3$  to  $6.0 \times 10^{22}$  el/s was performed during part of which the ELM frequency decreases from a value of 20-25 Hz (at lowest fuelling level) to 7-10 Hz, thus to the so-called type-I/II ELM regime at JET [5]. It was shown that with either  $N_2$  or Ne, conditions of partial divertor detachment were achieved with less than 10% energy confinement reduction in the main plasma with respect to low-fuelled reference case

( $\sim 0.3 \times 10^{22}$  el/s, #76666). A difference in the radiation localization was observed.  $N_2$  seeding increased the divertor radiation while Ne seeding decreased it. Also it was observed that the H-mode pedestal at the plasma edge of Ne-seeded discharges often crossed the boundary between type-I to III ELM regime, leading to compound ELMs and unsteady edge conditions. No condition was observed in this configuration for which  $N_2$ -seeding increased the plasma confinement, as was observed in ASDEX Upgrade with a full W-wall [6].

The transition from type-I to type-III ELM regime turned out to be the limitation in achieving a high value of divertor/X-point radiation over main plasma radiation with an H-factor close to 1. Figure 1 shows that when  $N_2$  is seeded in JET-C, at a rate from  $0.0$  to  $2.4 \times 10^{22}$  el/s, in the two plasma with highest density (#76684 and #76678), the pedestal density decreases followed by a decrease of both temperature and density at the highest seeding rate of  $\sim 4 \times 10^{22}$  el/s for which a transition from type-I to type-III ELM regime occurred.

## 3. Differences in confinement between JET-C and JET-ILW high-shape ELMy H-mode discharges at 2.5MA

Similar discharges were repeated in JET-ILW with practically identical high-shape (2.5MA/2.7T) with the aim to characterize the difference between JET-C and JET-ILW. Studies have shown that C concentration has dropped in the divertor and main plasma by a factor 10 [7]. Although dedicated studies address specific issue related to a change of material (such as divertor detachment, W erosion, impurity composition), the experiments presented here integrate all the aspects and provide a comparison with JET-C of the overall impact of

the new PFCs on the chosen plasma scenario. As expected, W contamination in the main plasma makes operation at low fuelling difficult and high-shape ELMy H-mode at 2.5MA is restricted to fuelling levels higher than  $0.9 \times 10^{22}$  el/s [8] in contrast to the lowest fuelling of  $\sim 0.3 \times 10^{22}$  el/s in JET-C related studies. In any case, studies made in JET-C in preparation for the change of Plasma Facing Components provides a good set of reference discharges for higher fuelling levels (up to  $6 \times 10^{22}$  el/s).

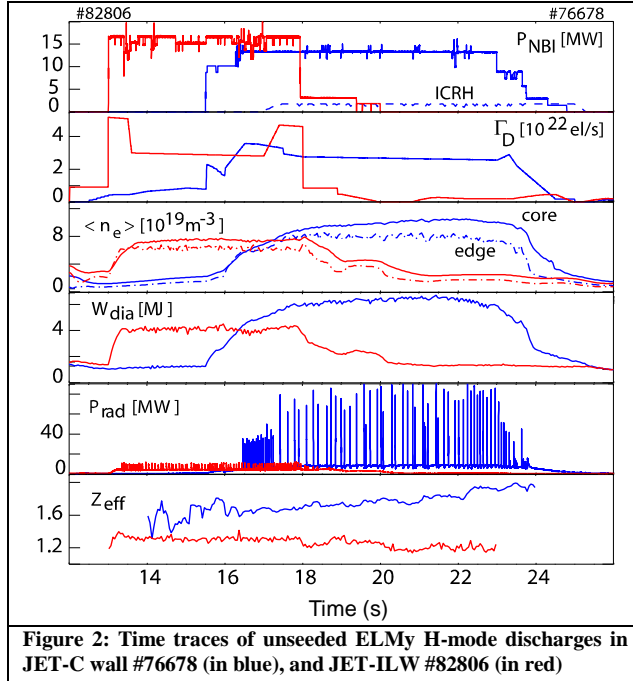


Figure 2: Time traces of unseeded ELMy H-mode discharges in JET-C wall #76678 (in blue), and JET-ILW #82806 (in red)

A comparison between JET-C (#76678) and JET-ILW (#82806) plasma at 2.5MA at a D<sub>2</sub>-fuelling rate of  $\sim 2.7 \times 10^{22}$  el/s is shown in Figure 2. At similar average electron density, and similar input power, the stored energy of the JET-ILW discharge is reduced by 40% in comparison to JET-C with a stored energy of 3.8MJ instead of 6.3MJ. The total radiative power has clearly decreased and the radiative fraction has dropped from 0.45 to 0.30. The radiative power from the bulk plasma and divertor is reduced in comparison to the JET-C reference discharge, by 1.4MW and 2.1 MW respectively. In JET-ILW, the plasma is cleaner with  $Z_{\text{eff}}$  reduced from 1.74 to 1.30 owing to the main impurity being

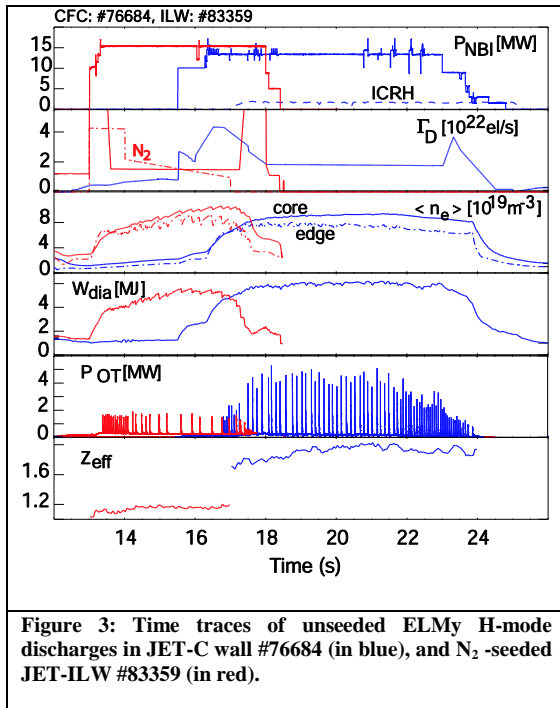
now Be instead of C. The neutral pressure in the sub-divertor is similar in both discharges. It is clear that the drop in confinement in the JET-ILW plasma compared to the JET-C one cannot be attributed to an increased main plasma radiation due to W. In fact, it stems from a drop in pedestal confinement. As shown in Figure 1, the electron temperature has dropped from a value of 0.6keV down to 0.4keV. More generally, similar plasmas within a fuelling range of 0.9 to  $3.2 \times 10^{22}$  el/s in the ILW covers a similar range of pedestal electron density as in JET-C, as shown in Figure 1, but the pedestal electron temperature is 30-40% lower on average. Although a reduction of the operational window was foreseen if main plasma radiation increased due to W contamination, this impact of the ILW on the confinement was unexpected.

Even more surprising is the fact that in JET-ILW type-I ELMs plasma, such as #82806, exists below the critical electron temperature of type-III ELMs in the JET-C at high density [9]. These plasmas have benign ELMs which are slower than anything noted before [1] and seem to exist in the pedestal  $n_e$  and  $T_e$  space which in JET-C would have been occupied by the type-III ELM regime. The ELM stability regime seems to have changed significantly. The boundary between the type-I to type-III ELM regime which was such a key player in both the ELM dynamics and drop in confinement in JET-C discharges as a result of seeding is not yet fully characterized for JET-ILW but lies far below its previous position.

#### 4. Recovery of confinement with N<sub>2</sub> seeding in high-shape ELMy H-mode discharges

In addition to increasing the radiative power, nitrogen seeding has been found to improve plasma energy confinement in high-shape ELMy H-mode. Figure 3 shows time traces of comparable plasmas, seeded with N<sub>2</sub> in JET-ILW and an unseeded JET-C reference

case at similar pedestal density. When nitrogen is injected into deuterium-fuelled discharges in JET-ILW, it raises the pedestal density and temperature leading to an increase in stored



energy to 5.5MJ close to the JET-C D<sub>2</sub>-fuelled counterpart, i.e. #76684 with 5.8MJ. The ELM frequency drops from ~16Hz to 4Hz is a result of seeding (was 9Hz for #76684). Without seeding, ELM crashes are slow and lead to benign power load on the divertor. With N<sub>2</sub> seeding, however, the ELM crashes speed up again and make the ELMs resemble more those seen with the carbon wall, as shown in Figure 3. The ELM power loads measured with Infra-red diagnostics on the outer divertor target are now comparable to JET-C plasmas. For the range of fuelling level of 0.8-3.0x10<sup>22</sup> el/s, it can be seen in Figure 4a that nitrogen seeding allows access to higher electron pedestal temperatures, only slightly lower than deuterium-fuelled JET-C counterparts. This leads to stored energies and H-factors only slightly below their deuterium-fuelled counterparts as seen in Figure 5a, and a very good match to JET-C N<sub>2</sub>-seeded pulses at similar nitrogen seeding rates, particularly when the density dependence is removed from the ITERH98(y,2) H-factor scaling, as shown in Figure 5b. The electron density of seeded discharges tends to be higher in JET-ILW than JET-C for same seeding level. The best N<sub>2</sub>-seeded pulse with the JET-ILW gives H<sub>98</sub>~0.92, n/n<sub>GW</sub>~1 with Z<sub>eff</sub>~1.5. The plasma stationarity is not achieved however and is addressed in section 6.

This is the first time in JET that injection of impurities leads to an increase in global energy confinement. Such a strong correlation between nitrogen seeding rate and stored energy has already been observed in AUG-Upgrade and is reported to be linked to a positive correlation between H-factor and Z<sub>eff</sub> [6]. In JET-ILW, such a clear dependence with Z<sub>eff</sub> has not been demonstrated. It is also important to note that the increase in confinement as a result from nitrogen injection in the ILW stems from the pedestal and not from an improved energy and particle confinement in the core plasma as proved by density and temperature peaking remaining unaffected.

The JET-ILW results strongly suggest that the carbon impurities played a role in the performance of the high-shape plasma scenario in the JET-C era. This is all the more striking if a closer look is taken at the plasma trajectory in the pedestal T<sub>e</sub>-n<sub>e</sub> diagram following N<sub>2</sub> injection together with the increase of divertor radiation and pedestal confinement, as shown in Figure 4a,4b. Focusing on the two highest fuelling levels in the JET-C plasmas, one can see that as N<sub>2</sub>-seeding rate is increased, the divertor radiation rises as expected and the pedestal confinement is slightly reduced up to the transition to type-III ELMs regime where the pedestal confinement drops by 20% at the highest divertor radiation. In comparison for JET-ILW plasmas as nitrogen seeding rate is increased, the divertor radiative power is raised and the pedestal confinement increases up to values similar to those in the deuterium fuelled JET-C counterparts. Once the maximum pedestal pressure has been achieved with nitrogen seeding, a further raise in seeding level leads to a decrease in density and a weaker decrease in temperature as shown in Figure 4a,4b, very like the trajectories of plasmas in JET-C with N<sub>2</sub>-seeding. These observations indicate that C level and associated radiation may have been a hidden parameter in the JET-C confinement behaviour in high-shape fuelled discharges, and

that the injection of  $N_2$  in JET-ILW partially recovers this effect. The exact mechanism is unknown. It remains to be identified whether the effect is directly linked to divertor radiation, or results from the ion dilution, or change in resistivity or local current density or turbulence suppression.

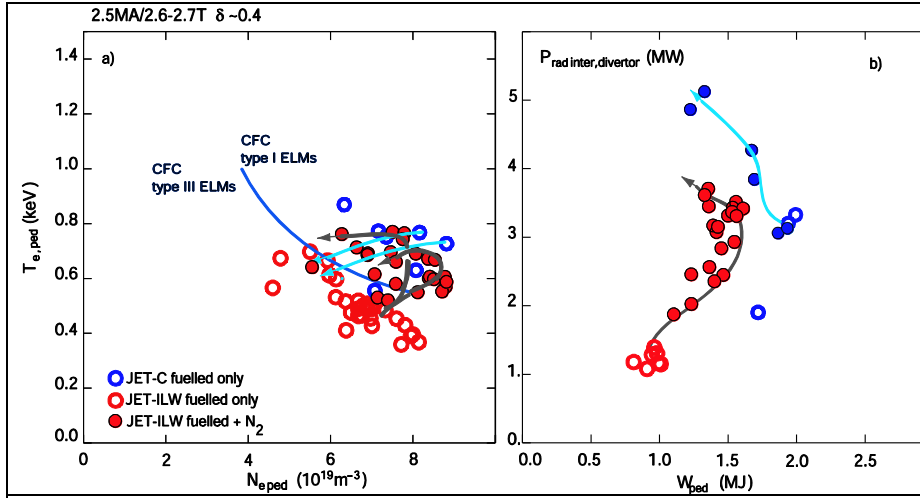


Figure 4: Pedestal trajectory as a result of seeding in  $T_e$ - $n_e$  diagram a) and divertor radiation inter-ELM versus pedestal confinement b)

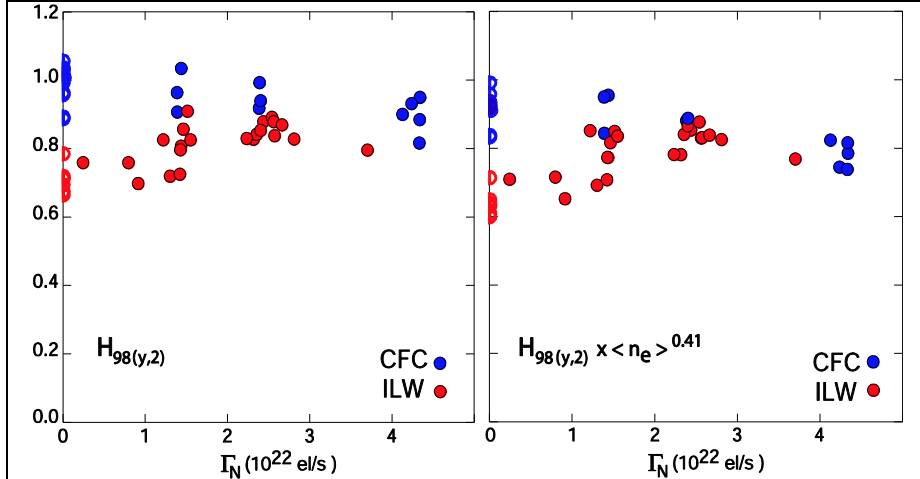


Figure 5: Dependence of normalized confinement with  $N_2$ -seeding rate: {on left} with the  $H_{98(y,2)}$  density scaling and (on right) with the density scaling removed.

with wide scan from  $0.3$  to  $6 \times 10^{22} el/s$ . In the JET-ILW, a more restricted range of fuelling ( $0.9$ - $3.2 \times 10^{22} el/s$ ) has so far been investigated. Nevertheless, these experiments provide the first comparison for ELMy H-mode discharges between JET-ILW and JET-C. For similar

## 5. Inter-ELM power load reduction in JET-ILW high $\delta$ discharges

With the reduction of C in the ILW, the resulting reduced divertor radiation is expected to lead to higher divertor power loads and higher electron temperature at the outer target in the inter-ELM periods.

In JET-C, with  $D_2$ -fuelling only, divertor conditions were probed from attached to high recycling

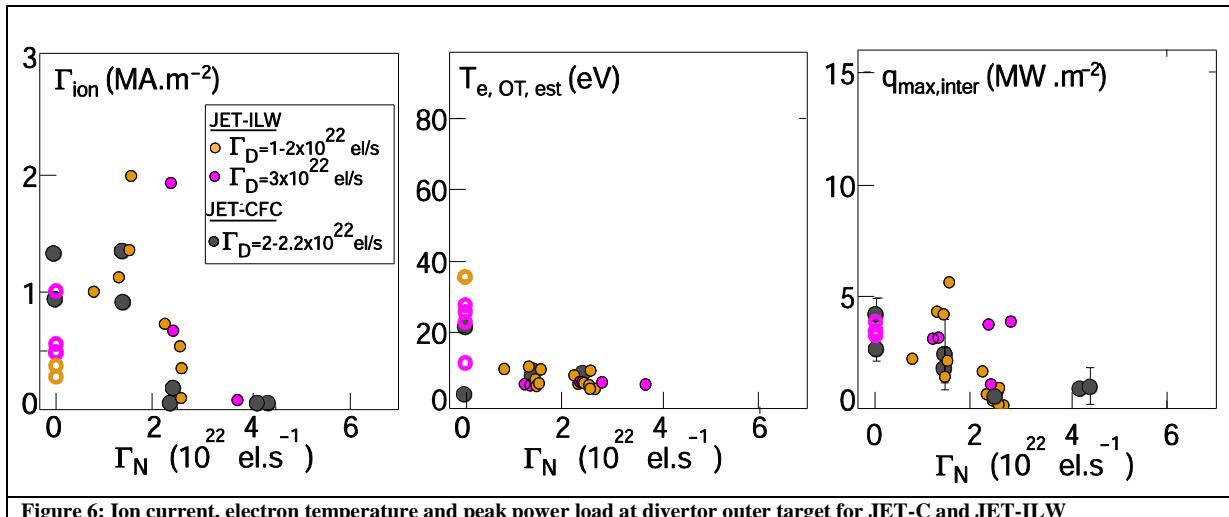


Figure 6: Ion current, electron temperature and peak power load at divertor outer target for JET-C and JET-ILW

power entering the Scrape-Off Layer (SOL), the electron temperature at the outer target is about  $\sim 36\text{eV}$  for the fuelling level of  $0.9 \times 10^{22}\text{el/s}$  and not too dissimilar to the value of  $\sim 40\text{--}55\text{eV}$  at the fuelling level of  $0.3 \times 10^{22}\text{el/s}$  obtained in JET-C. As the fuelling is increased through  $0.9$ ,  $2.8$  and  $3.2 \times 10^{22}\text{el/s}$ , the electron temperature decreases respectively as  $\sim 36\text{eV}$ ,  $26\text{eV}$  and finally  $12\text{eV}$  (no figure presented here). The peak ion current barely increases and the peak power load measured with the divertor Langmuir probes (LP) remains constant.

With  $\text{N}_2$ -seeding, a more substantial dataset is available for characterizing the divertor conditions between JET-ILW and JET-C. The measurements confirm that as nitrogen is injected in the plasma, divertor behaviour similar to the JET-C  $\text{N}_2$ -seeded discharges is recovered. On average the ion current rolls-over at a similar nitrogen seeding rate of  $\sim 2.5 \times 10^{22}\text{el/s}$  to that in JET-C, as shown in Figure 6. The electron temperature is then reduced to  $\sim 5\text{eV}$  and the peak power load is close to zero, see Figure 6. In fact, partial divertor detachment is obtained at the  $\text{N}_2$  seeding rate of  $2.5\text{--}3.7 \times 10^{22}\text{el/s}$  and with fuelling rate from  $0.8$  and  $2.9 \times 10^{22}\text{el/s}$ . Such a plasma corresponds to a factor  $H_{98} \sim 0.88$  (without removal of the density dependence),  $n/n_{\text{GW}} \sim 0.88$  and  $Z_{\text{eff}} \sim 1.8$ . The inter-ELM power load measured with IR was available for two of the seeded discharges and show discrepancy with the LP data. This discrepancy will be investigated.

## 6. Stationarity of plasma and average W erosion yield

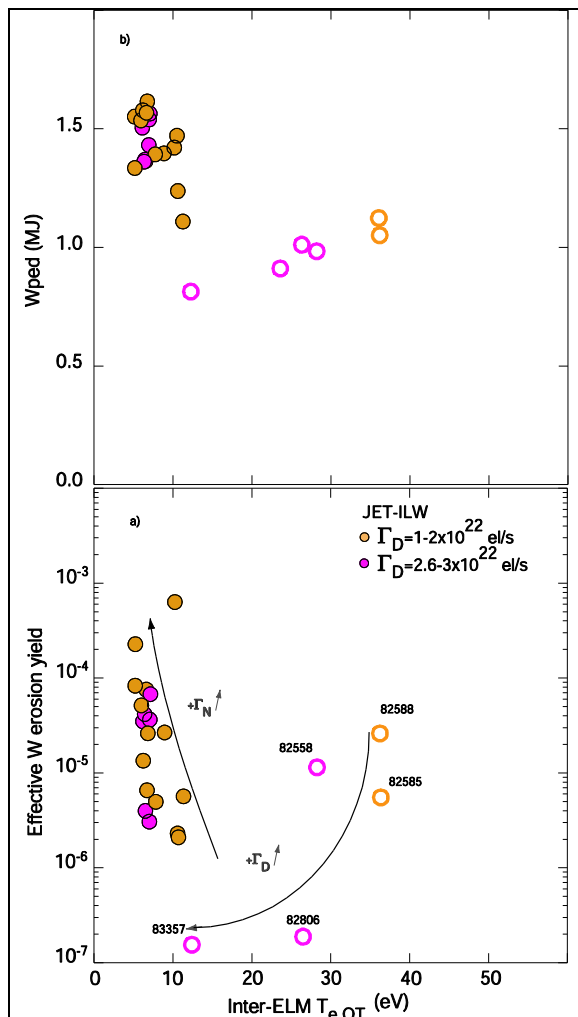


Figure 7: Effective W erosion yield a) and average pedestal stored energy versus target electron temperature in inter-ELM period b).

The W release is governed by impurity ions due to their threshold energy for W sputtering being an order of magnitude lower than that for deuterium. The sputtering yield for impurity ions such as  $\text{C}^{4+}$ ,  $\text{Be}^{2+}$ ,  $\text{N}^{4+}$  rises dramatically for plasma temperature above  $\sim 5\text{eV}$  [10,11]. At  $\sim 5\text{eV}$ , it is expected that no W will be sputtered by low Z impurities between ELMs. Tungsten will, however, still be sputtered by ELMs.

In these experiments, W erosion was measured by means of passive emission spectroscopy. The WI line radiation at  $400.9\text{nm}$  is monitored by a mirror-link system [12] with a time resolution of  $40\text{ms}$ , mostly able to provide an ELM-averaged measurement. The measured light intensities were transformed into W particle flux densities using the number of ionization per emitted photons, i.e.  $S/XB$  value as in reference [13]. The effective erosion yield is then obtained by normalization of the ELM-averaged peak W particle flux to the saturation current measured by LP. Results are shown in Figure 7. It can be seen that for fuelled only plasma (open symbol) where the pedestal pressure is weak and ELM benign, the erosion does decrease with target temperature as would be expected for an averaged erosion dominated by the inter-ELM phase. When  $\text{N}_2$  is seeded, the effective erosion increases even though the



electron temperature is decreased to value of  $\sim 5\text{eV}$ , thus all sputtering is due to high energetic ions hitting the target plate [13]. ELM energy density load responsible for material erosion is directly related to the pedestal pressure [14]. In fact the increased erosion yield at low target temperature is directly linked to an increase in pedestal confinement and therefore pressure as shown in Figure 7. In other words, as nitrogen is seeded and the pedestal confinement increases, the W erosion yield is governed by the ELMs and not the inter-ELM phase. Previous studies in  $\text{D}_2$ -fuelled discharges (in which Be is the main impurity responsible for W sputtering) have shown that the intra-ELM W sputtering dominated by a factor 5 over the inter-ELM phase [14]. In our discharges, N is present and is a heavier an impurity than Be and is expected to sputter W more than Be during an ELM.

The  $\text{N}_2$ -seeded high  $\delta$  ELMy H-mode considered provides the first case in JET-ILW of a scenario with power load control though high ELM energy density loads together with long enough plasma duration to probe the impact of W on plasma confinement and stationarity. Time traces of a typical  $\text{N}_2$ -seeded discharge with  $H_{98}\sim 0.9$ ,  $n/n_{\text{GW}}\sim 1$  and  $Z_{\text{eff}}\sim 1.5$  are shown in Figure 8. This figure illustrates that  $\text{N}_2$ -seeded high- $\delta$  ELMy H plasmas with higher confinement so far have an unstationary behaviour. Although the total radiative power and energy confinement are constant over most of the plasma duration, the core electron temperature decreases, while the plasma radiation within the sawtooth inversion radius increases. Once the sawteeth disappears, the core radiation increases exponentially. W is

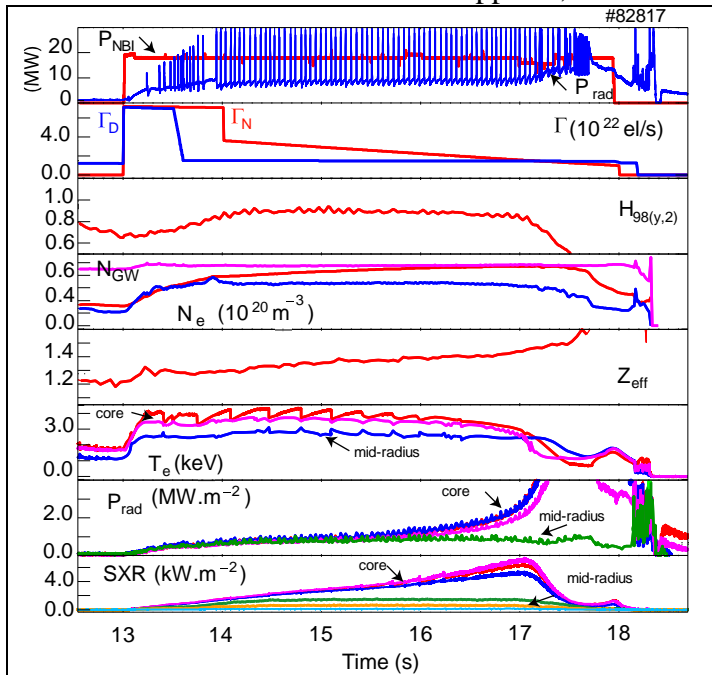


**Figure 8: Time traces of  $\text{N}_2$ -seeded ELMy H-mode discharges in JET-ILW wall #82817** (from top to bottom) NBI heating and total radiated power,  $\text{D}_2$  and  $\text{N}_2$  waveforms, normalized confinement factor  $H_{98}$ , core (red) edge (in blue) and Greenwald electron density (in pink), line-integrated  $Z_{\text{eff}}$ , electron temperature from core (in red and pink) and mid-radius (in blue), radiated power from core (in blue and pink) and mid-radius (in green) channel, and finally Soft x-ray radiated power.

accumulating in the very plasma centre (within  $\rho\sim 0.3$ ) and when the plasma enters its termination phase leads to high radiative power and finally a disruption. It is important to note that high- $\delta$  ELMy H-modes were not stationary in JET-C either with a  $Z_{\text{eff}}$  constantly increasing as shown in Figure 2. In fact, ICRH was added to neutral-beam heating as an integral part of the scenario for control of density peaking and sawteeth [5,16]. In the JET-ILW discharge, first test with ICRH heating in this scenario did not show any benefit so far. The density peaking outside the ST radius is the same in ILW as in JET-C. As a result, it could be that the impurity peaking is similar to what was observed in the JET-C, just made more evident by the presence of an additional and much higher Z impurity such as W.

To develop a long discharge of about 20s flat-top it is essential to improve the plasma stationarity by reducing first W penetration through the separatrix and second W peaking inside the main plasma. The first point needs to be addressed by a reduction of the W source or transport both of which can be addressed with different divertor configurations. The second point is likely to require the use of core heating for either controlling the ST behaviour or some possible beneficial outward turbulent convection.

## 7. Lack of improved confinement with N<sub>2</sub> seeding in other configurations

Observations presented above have indicated that C level and associated radiation may have been a hidden parameter in the JET-C confinement behaviour in high-shape fuelled discharges. This could be why such discharges in JET-ILW have a ~40% decrease in confinement compared to the JET-C counterpart, and why the injection of N<sub>2</sub> partially recovers this confinement. In contrast, it is not believed that C radiation is a hidden parameter for low- $\delta$  ELMy H-mode discharges. Their confinement is reported to be comparable in JET-ILW and JET-C, the only difference being that low fuelling operation, favourable for high H-factor, is no longer accessible due to W contamination in the main plasma. Nevertheless as a mean to gather further evidence on the effect of nitrogen, this seed impurity was injected into low- $\delta$  ELMy H-mode at 2.5MA and similar divertor geometry. A low- $\delta$  ELMy H-mode with vertical targets, more similar to the ITER divertor geometry, was also tested. No increase in confinement with N<sub>2</sub>-seeding was observed. The range of  $Z_{\text{eff}}$  values covered with the low  $\delta$  configuration was from 1.2 to 1.5 and similar to that of the high  $\delta$  configuration (1.1-1.8), demonstrating the lack of dependence of confinement on  $Z_{\text{eff}}$  value. It also suggests a possible role of divertor radiation in high-shape ELMy H-mode plasma at JET.

The vertical target configuration proved interesting for two reasons. First the W contamination in the main plasma was much reduced and the operational window seemed to extend to very low fuelling close to levels used in JET-C. Very first results show signs of a higher stored energy with no additional fuelling but further work is needed to confirm this. Second, W events occurring fairly frequently with the horizontal target divertor configuration but with the vertical target none were observed so far.

## 8. Conclusion

It was expected that the change from CFC to the ILW at JET would limit the operational window to higher fuelling levels both for low- and high-shape ELMy H-mode discharges, in order to keep the W contamination and induced radiation low in the main plasma. However, it was not anticipated that the new plasma-facing components would reduce the pedestal confinement of high-shape ELMy H-mode in comparison to the JET-C counterpart. The injection of an extrinsic impurity, N<sub>2</sub>, in high- $\delta$  ELMy H-mode was shown to recover the pedestal confinement. This paper suggests that C level and associated radiation could have been a hidden parameter in the JET-C confinement behaviour of high shaped plasma and that N<sub>2</sub> partially recovers this effect in JET-ILW. The exact mechanism has not been identified so far. It was shown that once the pedestal pressure of typical discharges in JET-C is mostly recovered, the ELM governs the averaged W erosion yield. Operation at high H-factor and high density is paramount for JET-ILW and ITER. The next step for the development of the JET-ILW compatible scenarios will be to integrate techniques to control plasma stationarity to open-up the operational space to long pulse and high current operation.

[1] Matthews G. et al, PSI 2012 to be published

[2] Oberkofler M. et al, PSI 2012 to be published

[3] Maddison G.P. et al, Nucl. Fusion **51** (2011) 042001

[4] Giroud C. et al., Nucl. Fusion **52** (2012) 063022

[5] Saibene G. et al 2002 Plasma Phys. Control. Fusion **44** 1769–99

[6] Schweinzer J. et al 2011 Nucl. Fusion **51** 113003

[7] Brezinsek S. et al., PSI 2012 to be published

[10] Eckstein W. et al 1993 Nucl. Instrum. Methods B **83** 95

[11] Thomas A. et al 1997 Plasma Phys. Control. Fusion **39**

[12] Meigs A. et al, PSI 2012, JNM to be published

[13] Brezinsek S. et al., Phys. Scr. T145 (2011) 014016.

[14] van Rooij G., this conference

[15] Thomsen H. et al, Nucl. Fusion **51** (2011) 123001

[16] Nave M.F.F. et al 2003 Nucl. Fusion **43** 1204–13

*This work, supported by the European Communities under the contract of Association between EURATOM and CCFE, was carried out within the framework of the European Fusion Development Agreement. The views and opinions expressed herein do not necessarily reflect those of the European Commission. This work was also part-funded by the RCUK Energy Programme under grant EP/I501045*